# Session C

# Convection

https://doi.org/10.1017/S0074180900133303 Published online by Cambridge University Press

*Modelling of Stellar Atmospheres*
*IAU Symposium, Vol. 210, 2003*
*N. E. Piskunov, W. W. Weiss, D. F. Gray, eds.*

# Energy Transport, Overshoot, and Mixing in the Atmospheres of Very Cool Stars

Hans-Günter Ludwig

*Lund Observatory, Box 43, 22100 Lund, Sweden; hgl@astro.lu.se*

**Abstract.** We constructed hydrodynamical model atmospheres for mid M-type main-, as well as pre-main-sequence objects. Despite the complex chemistry encountered in such cool atmospheres a reasonably accurate representation of the radiative transfer is possible. The detailed treatment of the interplay between radiation and convection in the hydrodynamical models allows to study processes usually not accessible within the framework of conventional model atmospheres. In particular, we determined the efficiency of the convective energy transport, and the efficiency of mixing by convective overshoot. The convective transport efficiency expressed in terms of an equivalent mixing-length parameter amounts to values around $\approx 2$ in the optically thick, and $\approx 2.8$ in the optically thin regime. The thermal structure of the formally convectively stable layers is little affected by convective overshoot and wave heating, i.e. stays close to radiative equilibrium. Mixing by convective overshoot shows an exponential decline with geometrical distance from the Schwarzschild stability boundary. The scale height of the decline varies with gravitational acceleration roughly as $g^{-\frac{1}{2}}$, with 0.5 pressure scale heights at $\log g{=}5.0$.

## 1. Introduction

The increasing number of late M-type stars, brown dwarfs, and extrasolar planets discovered by infrared surveys and radial velocity searches has spawned a great deal of interest in the atmospheric physics of these objects. Their atmospheres are substantially cooler than e.g. the solar atmosphere, allowing the formation of molecules, or even liquid and solid condensates. Convection is a ubiquitous process in these atmospheres shaping the thermal structure and the distribution of material. Hydrodynamical simulations of solar and stellar granulation including a realistic description of radiative transfer have become an increasingly powerful and handy instrument for studying the influence of convective flows on the the structure of late-type stellar atmospheres as well as on the formation of their spectra. Here we report on efforts to construct hydrodynamical models for mid M-type atmospheres. We consider this as an intermediate step on the way to model brown dwarf and planetary atmospheres. The motivation was twofold: Firstly, pre-main-sequence evolutionary models of M-dwarfs and brown dwarfs based on mixing-length theory (MLT) depend sensitively on the mixing-length parameter $\alpha_{\rm MLT}$ (Baraffe et al. 2002). Secondly, the distribution of dust clouds in brown dwarfs depends on the efficiency of mix-

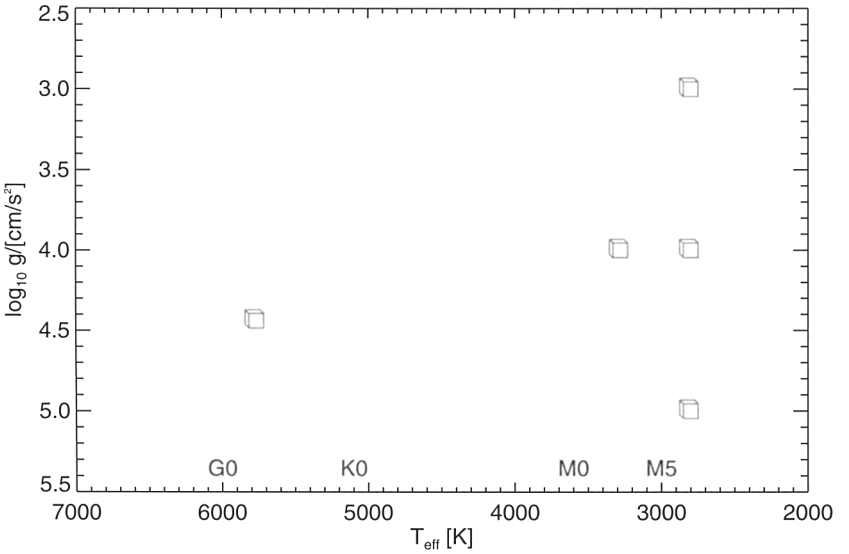


Figure 1. The radiation-hydrodynamics models in the effective temperature-gravity plane (cubes). The approximate spectral class is indicated at the temperature axis.

ing by convective overshoot. Conventionally, convection is described within the simplistic picture of MLT dependent on free parameters. Our hydrodynamical models provide a description essentially from first principles free of the uncertainties of MLT, putting stellar models on a firmer footing.

## 2. Model overview

Figure 1 illustrates in the location of the hydrodynamical model atmospheres considered in this investigation in the $T_{\rm eff}$-log g-plane: three M-type models are located at $T_{\rm eff}$=2800 K with log g=3.0, 4.0, and 5.0 which form a log g-sequence. To assess the temperature effects a somewhat hotter M-type model is located at $T_{\rm eff}$=3280 K and log g=4.0. For comparison we also considered a solar model at $T_{\rm eff}$=5777 K, log g=4.44. All models possess solar chemical composition.

The RHD simulations were performed with a convection code developed by Å. Nordlund and. R.F. Stein (see Stein & Nordlund 1998, and references therein). The code implements a consistent treatment of compressible gas flows together with non-local radiative energy exchange in three spatial dimensions. The radiative transfer is treated in LTE approximation, the wavelength dependence of the radiation field is represented by a small number of wavelength bins. Open lower and upper boundaries, as well as periodic lateral boundaries are assumed. The effective temperature of a model (i.e. the average emergent radiative flux) is controlled indirectly by prescribing the entropy of inflowing material at the lower boundary. Magnetic fields are neglected. Opacities and

https://doi.org/10.1017/S0074180900133303 Published online by Cambridge University Press

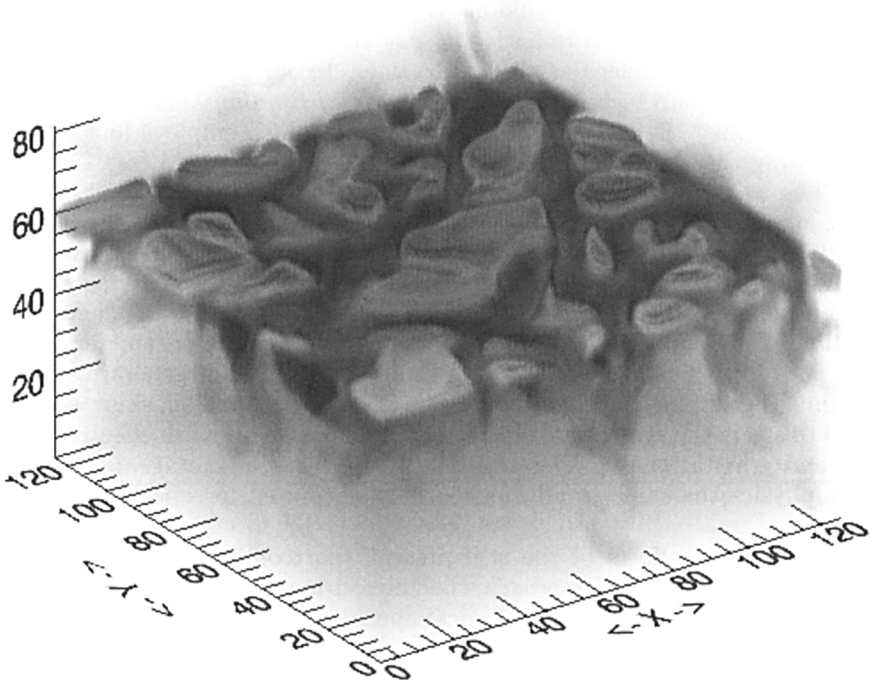


Figure 2. Typical temperature field during the evolution of a 3D hydrodynamical model of a late-type atmosphere. Lighter shades of gray correspond to higher temperatures.

equation-of-state have been adapted to the conditions encountered in the M-type atmospheres. In particular, the equation-of-state accounts for $H_2$ molecule formation, the opacities include contributions of molecular lines. The opacities were extracted from the opacity data base of the PHOENIX model atmosphere code (for a description of the code see Hauschildt & Baron 1999). The application of the Nordlund & Stein convection code to M-type objects in described in more detail in Ludwig, Allard, & Hauschildt (2002, hereafter LAH).

Figure 2 visualizes the flow structure (here via the temperature field) generically encountered in our hydrodynamical models for late-type stars. The computational domain is a Cartesian box representing a small volume at the stellar surface. It comprises the optically thin photospheric layers as well the uppermost layers of the convection zone which extends deeper into the star. A granulation pattern is visible in layers around optical depth unity. Concentrated, plume-like downdrafts dominate the sub-photospheric flow, the optically thin layers are harbouring a mixture of overshooting and wave motions with associated temperature fluctuations.

We want to derive quantitative estimates of the mixing by convective overshoot, as well as obtain a measure of the efficiency of the convective energy

https://doi.org/10.1017/S0074180900133303 Published online by Cambridge University Press

transport. For addressing these issues the RHD models have to give a reasonably accurate representation of the actual atmospheric conditions. Here we are particularly concerned about the radiative energy transport, which is complicated by the huge number of molecular absorption lines. In our hydrodynamical models we use a multigroup technique (dubbed *Opacity Binning Method*, hereafter OBM) for modelling the radiative energy exchange which employs four groups for representing the wavelength dependence of the radiation field (see LAH for details). The wavelength groups have been optimised for the $T_{\rm eff}$=2800 K and $\log g$=5.0 model. Figure 3 illustrates the accuracy which is achieved with the OBM. While there are differences between the atmospheric structure based on the OBM and PHOENIX models, which are based on direct opacity sampling, the OBM provides a significant improvement with respect to the simple grey approximation. Differences increase as one chooses atmospheric parameters away from the ones for which the OBM was optimised. We did not generate specifically optimised groupings for all atmospheres under consideration, since we were interested to study the systematic change of model properties with effective temperature and gravitational acceleration. I.e it appeared advantageous to leave the input physics the same in all models, only optimised for one temperature and gravity.

To mitigate the effects of the still present shortcomings in the radiative transfer we took a *differential approach* when measuring model properties: whenever possible we compared hydrodynamical and hydrostatic model atmospheres based on the same radiative transfer scheme, i.e. here the OBM.

## 3. Granulation in M-type objects

Our small sample of hydrodynamical M-type atmospheres gives some insight into the properties of stellar granulation at cooler temperatures. Figure 4 compares the granulation pattern of the $T_{\rm eff}$=2800 K, $\log g$=3.0 model with the one of a solar model. The first thing to note is that surface convection in M-type objects produces a granular pattern qualitatively resembling solar granulation: bright extended regions of upstreaming material which are surrounded by dark concentrated lanes of downflowing material. The dark lanes form an interconnected network. Looking more closely, granules are less regularly delineated in M-type objects, the inter-granular lanes show a higher degree of variability in terms of their strength. A feature which is uncommon in the solar granulation pattern are the dark "knots" found in or attached to the inter-granular lanes. The knots are associated with strong downdrafts which carry a significant vertical component of angular momentum. The width of the inter-granular lanes to the typical granular size is smaller in our M-type objects. Inspecting the velocity field (not shown) in vicinity of the continuum forming layers shows less pronounced size differences. This indicates that the relatively broader lanes in the solar case are the result of a stronger smoothing of the temperature field due to a more intense radiative energy exchange, i.e. the effective Peclét number of the flow is larger around optical depth unity in the cooler objects.

https://doi.org/10.1017/S0074180900133303 Published online by Cambridge University Press

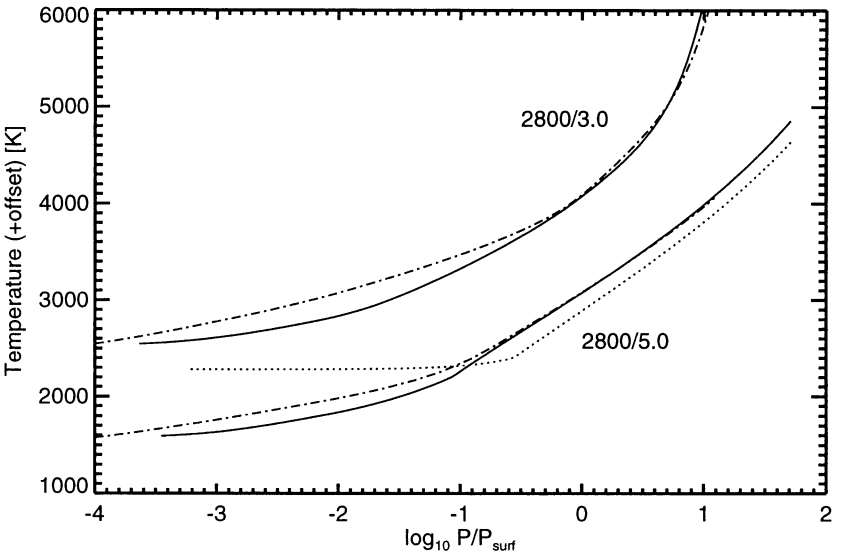


Figure 3. Comparison of the pressure-temperature structure between 1D hydrostatic model atmospheres in radiative-convective equilibrium based on the OBM (solid lines) with 4 wavelength groups, and PHOENIX models based on direct opacity sampling employing several 10 000 wavelength points (dash-dotted). Shown are two examples with $T_{eff}$=2800 K and log g=3.0 and 5.0, respectively. For clarity, the log g=3.0 models were shifted by +1000 K. Also shown is a model employing grey radiative transfer (dotted line). The pressure is given in units of the pressure at Rosseland optical depth unity $P_{surf}$.

## 4. Mixing by atmospheric overshoot

Stellar atmospheres around $T_{eff} \approx 2800$ K are too hot to allow for a significant formation of dust grains. However, already at slightly cooler effective temperatures, grain formation sets in and dust grains become major opacity contributors, i.e. an important factor in determining the thermal structure of the atmosphere. In fact, the spectral energy distribution in the range of effective temperatures $1500\,\mathrm{K} \leq T \leq 2500\,\mathrm{K}$ is crucially linked to the distribution of dust grains in the atmosphere (e.g. Allard, Hauschildt, & Schwenke 2000). The amount of dust which is present is determined by chemical condensation and evaporation processes as sources and sinks, as well as macroscopic transport processes which carry dust grains away from their sites of formation. In M-type and cooler atmospheres the transport is dominated by two opposing processes: gravitational settling of dust grains and their mixing due to the presence of velocity fields, either related to convection or global circulations induced by rotation. In our models, no dust formation takes place but we nevertheless find it worthwhile to give a characterisation of the atmospheric mixing due to convection and con-

https://doi.org/10.1017/S0074180900133303 Published online by Cambridge University Press

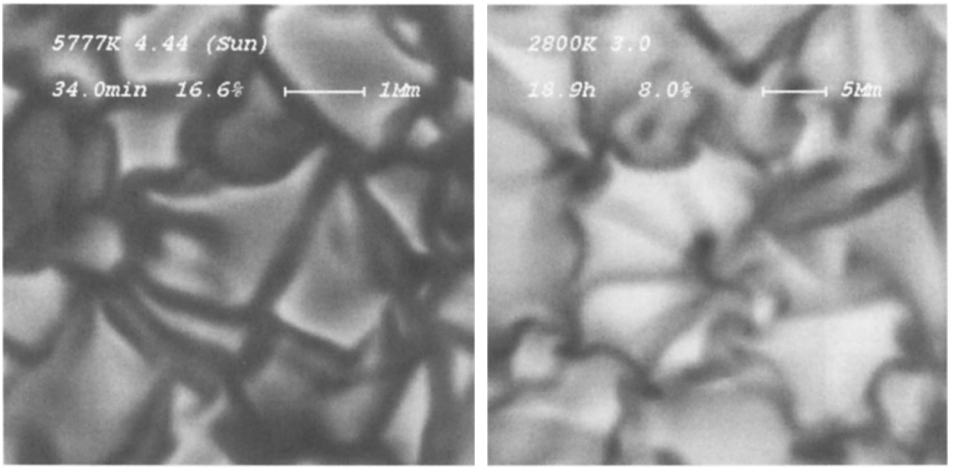


Figure 4. Granulation pattern in the solar model (left panel) and the $T_{\rm eff}$=2800 K, log g=3.0 M-type model (right panel). Shown is the emergent intensity in the continuum. At the particular instants in time the relative intensity contrasts amount to 16.6 % in the solar case, and 8.0 % in the M-type case. Note, the different spatial scales.

vective overshoot. This can give at least a first order approximation of how convective mixing might operate when dust is actually present.

Formally, we are interested in a statistical representation of the mean transport properties of the convective velocity field in vertical direction. The horizontal advection of dust grains by the convective velocity field probably produces horizontal inhomogeneities in the dust distribution. We neglect these here since i) we are targeting at the application of our results in standard 1D stellar atmosphere models, ii) the horizontal inhomogeneities are small scale (the size of a convective cell), i.e. hardly observable and iii) the uncertainties in our understanding of the dust formation process itself perhaps limits the achievable accuracy anyway. In view of the last point we present a proxy of the convective mixing only, without trying to derive a detailed statistical description of the transport properties of the convective velocity field, i.e. extracting its effective transport coefficients (c.f. Miesch, Brandenburg, & Zweibel 2000, for an example of a more stringent treatment).

As proxy measuring the mixing properties of the velocity field we introduce the mixing velocity $v_{\rm mix}$

$$v_{\rm mix} \equiv \frac{F}{\langle \rho \rangle} \tag{1}$$

($\rho$ denotes the mass density, $\langle . \rangle$ temporal and horizontal averaging) where $F$ is the temporally and horizontally averaged vertical gross mass flux

$$F \equiv \langle \rho u_{\rm z} \rangle_{\rm t,up} \tag{2}$$

($u_{\rm z}$ denotes the vertical velocity). For $F$ the average is taken over surface areas with upwards directed flow only. Note, that the average total mass flux vanishes.

https://doi.org/10.1017/S0074180900133303 Published online by Cambridge University Press

$F$ measures the amount of mass flowing in and out a certain layer. If the in- and outflow happens sufficiently disordered, this mass exchange goes hand in hand with mixing of material.

As we shall see below $v_{\rm mix}$ exhibits an exponential height dependence. With such an dependence a characteristic mixing frequency $f_{\rm mix}$ can be written as

$$f_{\rm mix} \equiv -\frac{1}{\langle\rho\rangle}\frac{dF}{dz} = v_{\rm mix}\left(\frac{1}{H_{\rm v}} + \frac{1}{H_\rho}\right), \tag{3}$$

where $H_{\rm v}$ denotes the scale height of $v_{\rm mix}$, and $H_\rho$ the density scale height.

### 4.1. Subsonic filtering

As mentioned previously, the atmospheric velocity field is a superposition of advective, overshooting motions and acoustic waves generated by convection in deeper layers (see also Ludwig & Nordlund 2000). The wave motions contribute little if at all to the mixing due to their spatially coherent, oscillatory character. The overshooting, convective motions tend to decay with distance from the Schwarzschild stability boundary, while the wave motions tend to increase in amplitude due to the exponential decrease of the density with increasing height. This leads to the situation that beyond a certain height the atmospheric velocity field is even dominated by wave motions. In order to get a reliable estimate of the mixing it is therefore necessary to remove the wave contributions to the velocity field before evaluating the gross mass flux $F$.

We removed the wave contributions by subsonic filtering — a technique invented in the context of solar observations for cleaning images from "noise" stemming from the solar 5 minute oscillations (Title et al. 1989). Figure 5 schematically illustrates this filtering technique. In short, one considers a time sequence of images and removes features with horizontal phase speeds $v_{\rm phase}$ greater than a prescribed threshold. This is achieved by Fourier filtering of spatial-temporal data in the $k$-$\omega$ domain. For every depth layer in our data cubes we performed a 3D Fourier analysis (one temporal, two spatial dimensions) of the vertical mass flux retaining only contributions below a preset velocity threshold. In practice, acoustic and convective contributions are not as cleanly separated as shown in the Fig. 5, and one must find the right balance between removing as much acoustic components as possible while retaining as much as possible convective contributions. We always studied a sequence of phase speed thresholds in order to judge the success of the procedure.

### 4.2. Mixing in the solar atmosphere

Despite we are not primarily interested in the Sun here, it is worthwhile to look at the Sun as a reference object to compare with. Figure 6 shows $v_{\rm mix}$ in our solar model for various degrees of subsonic filtering. It is clearly visible that the subsonic filtering has the strongest impact on $v_{\rm mix}$ in the uppermost atmospheric layers. As advertised before $v_{\rm mix}$ *exhibits an exponential decline with height* ($\log P \propto z$) *after appropriate subsonic filtering*. This feature was put forward by Freytag, Ludwig, & Steffen (1996) as generic feature of convective overshoot. Moreover, we see that too low a velocity threshold removes also convective features, as visible by the reduction of the velocity in the deeper,

https://doi.org/10.1017/S0074180900133303 Published online by Cambridge University Press

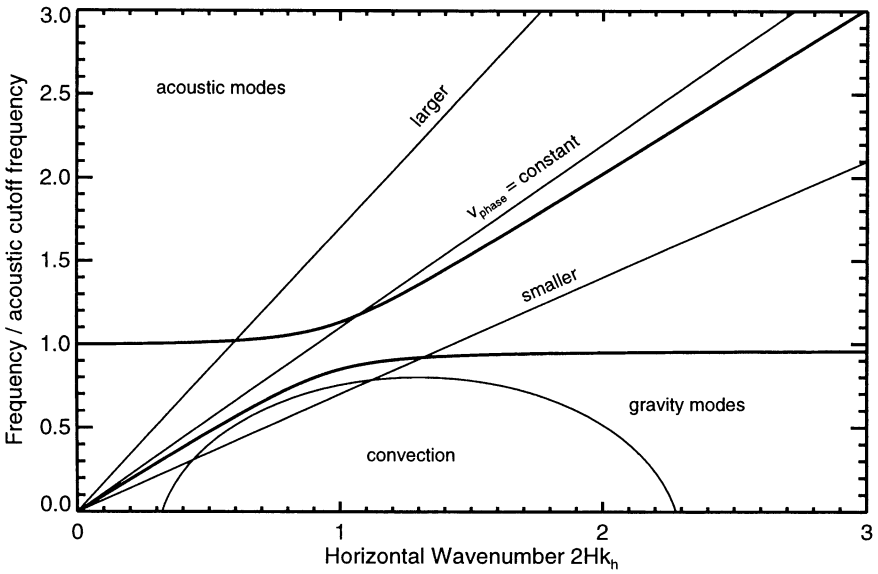


Figure 5. Schematic illustration of subsonic filtering: Only components in wavenumber-frequency domain below a prescribed phase speed $v_{\rm phase}$ are retained. They preferentially belong to convective motions.

convection dominated layers. Quantitatively, for the Sun we find that $H_{\rm v} = (1.9 \pm 0.2) H_{\rm p}$, where $H_{\rm p}$ denotes the local pressure scale height.

The exponential decline of $v_{\rm mix}$ is also motivated from studying linear convective modes. In Fig. 6 we plotted the velocity profiles of linear convective eigenmodes with horizontal wavelength of 1.5 and 5.0 Mm, respectively. We used the temporally and horizontally averaged hydrodynamical model as background mode. The absolute velocity amplitude of the modes has been scaled to match $v_{\rm mix}$ from the hydrodynamical model. We see that the velocity field of the modes exhibits an exponential "leaking" into the formally convective stable layers, and the decline is more rapid for the mode with shorter wavelength. We further see that the mode with 5 Mm wavelength shows a decline similar to the decline of $v_{\rm mix}$. Interestingly, the wavelength of the fitting mode is significantly larger than the horizontal scale of the dominant convective structures on the Sun — the granules with typical sizes of around 1.5 Mm.

### 4.3. Mixing in M-type atmospheres

Figure 7 shows $v_{\rm mix}$ for the M-type models at $T_{\rm eff}$=2800 K. With decreasing gravity the zone of convective instability extends further and further into the optically thin atmosphere, leaving little room for overshoot in the lowest gravity model. Reading off an exponential decline rate is very uncertain here. However, we find a slow decline with $H_{\rm v} \approx 6 H_{\rm p}$. For the $\log g$=4.0 model we find a value close to solar of $1.7\,H_{\rm p}$, for the $\log g$=5.0 model $0.5\,H_{\rm p}$. Qualitatively,

https://doi.org/10.1017/S0074180900133303 Published online by Cambridge University Press

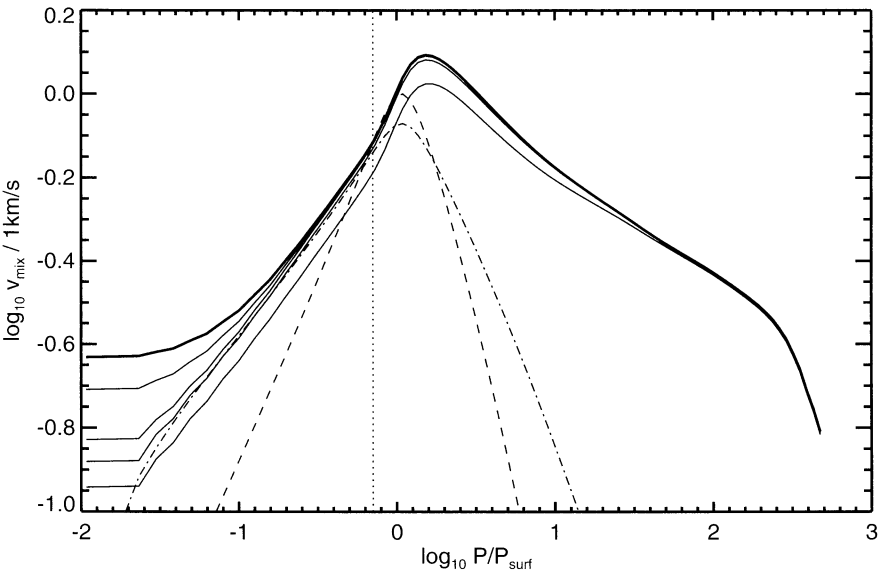


Figure 6. Mixing velocity in a solar model as a function of pressure: the unfiltered data (thick solid line) were subsonically filtered with $v_{\rm phase}$ = 12, 6, 3, and 1.5 km/s (thin solid lines from top to bottom). The approximate location of the Schwarzschild boundary of convective stability is indicated by the dotted line. The velocity profiles of convective eigenmodes with a horizontal wavelength of 1.5 Mm (dashed line) and 5.0 Mm (dash-dotted line) are also shown. The pressure is given in units of the pressure at Rosseland optical depth unity $P_{\rm surf}$. The velocity plateau at the upper boundary is a numerical artifact of the upper boundary condition of the hydrodynamical model.

overshooting is less pronounced in models of higher gravity. This is of course related to the fact that the buoyancy forces scale proportional to gravity, making buoyancy more effective in confining the convective motions to the formally unstable regions. Empirically we find that the scale height of $v_{\rm mix}$ roughly scales as $g^{-\frac{1}{2}}$.

Trying to match the velocity profile in the overshooting regions worked only partially. For the lower gravity models the fit is not very good which might be related the situation that convection reaches very high atmospheric layers. We oriented the horizontal wavelength of the linear modes at the largest sizes of structures the computational box could accommodate in the respective models.

## 5. The efficiency of the convective energy transport

Convection is an important energy transport mechanism in M-type stars. In standard model atmospheres it is treated in the framework of MLT. The question

https://doi.org/10.1017/S0074180900133303 Published online by Cambridge University Press

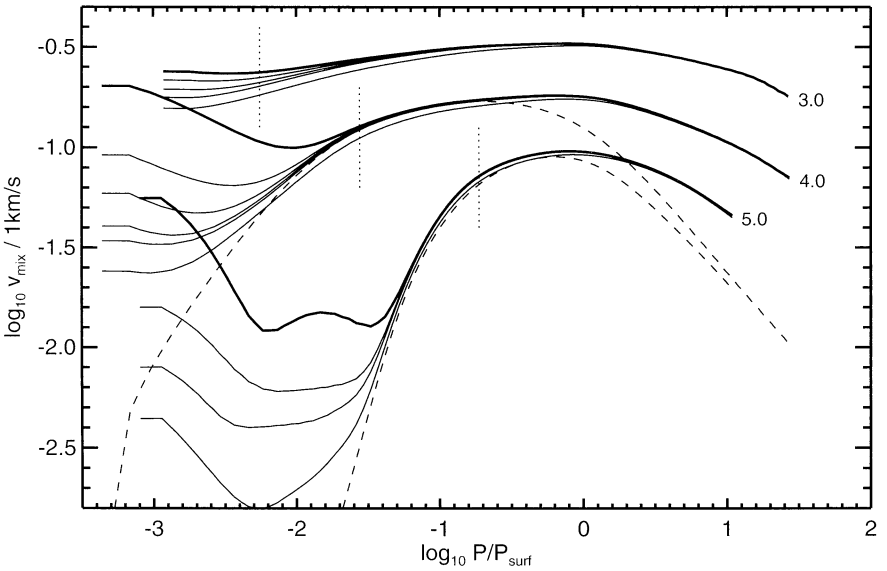


Figure 7. Mixing velocities in the M-type models with $T_{\rm eff}$=2800 K and log g=3.0, 4.0, and 5.0 (groups of solid lines, top to bottom) as a function of pressure: shown are the unfiltered data (thick solid lines) and subsonically filtered data (thin solid lines, top to bottom) with $v_{\rm phase}$= 8.0, 4.0, 2.0, 1.0 km/s (log g=3.0 and log g=4.0); 1.0, 0.5, 0.25 km/s (log g=5.0). The approximate locations of the Schwarzschild boundaries are indicated by the dotted lines. The dashed lines depict velocity profiles of convective modes with horizontal wavelength of 3.0 Mm (log g=4.0) and 250 km (log g=5.0).

is whether the simplistic MLT is actually capable to provide a reasonable description of the convective energy transport under conditions encountered in the M-type atmospheres. Figure 8 shows a comparison of the thermal structure of the hydrodynamical model atmospheres and standard 1D hydrostatic model atmospheres in radiative-convective equilibrium assuming different mixing-length parameters. The hydrodynamical models have been averaged temporally and horizontally on surfaces of constant optical depth. This procedure ensures a particularly good preservation of the energy transport properties of the hydrodynamical models (Steffen, Ludwig, & Freytag 1995). Besides the mixing-length parameter MLT contains a number of further "hidden" parameters intrinsic to the specific formulation of MLT which was chosen. We emphasise that a well-defined calibration of the mixing-length parameter must be always given with reference to the specific formulation. Here, we are using the formulation as given by Mihalas (1978).

The sensitivity of the structure of the standard models to the mixing-length parameter increases with decreasing gravity. This is in line with the earlier statement that stellar structure models depend sensitively on the mixing-length

https://doi.org/10.1017/S0074180900133303 Published online by Cambridge University Press

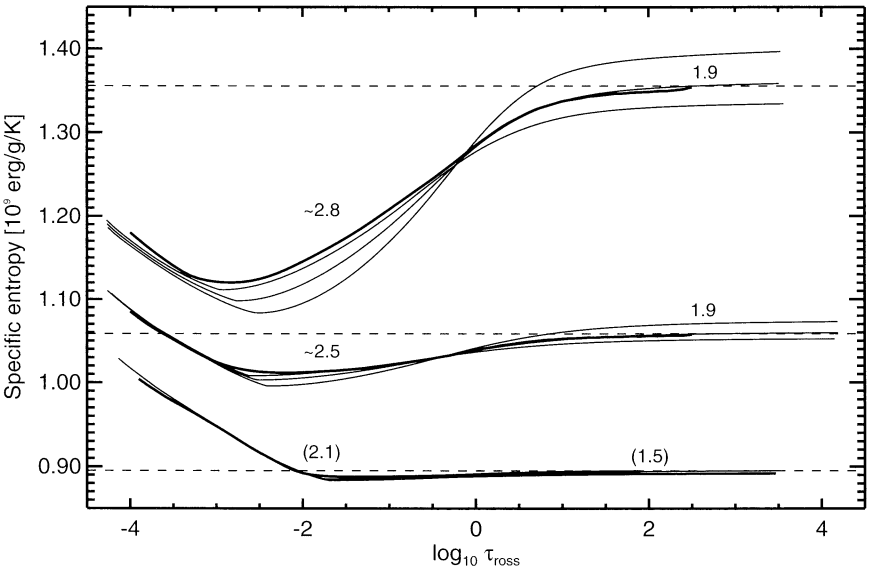


Figure 8. Entropy structure of the hydrodynamical models (thick solid lines; log g=3.0, 4.0, 5.0, top to bottom) in comparison to standard mixing-length models (thin solid lines). For each hydrodynamical model three MLT models are plotted with $\alpha_{\rm MLT}$=1.5, 2.0, and 2.5. The dashed lines depict an extrapolation towards the asymptotic entropy encountered deep in the convective zone. Numbers indicate approximate mixing-length parameters necessary to match the hydrodynamical structure with standard models.

parameter at lower gravities. Towards the main sequence the sensitivity is largely reduced making a precise calibration of $\alpha_{\rm MLT}$ difficult — but of course also less important. The M-type atmospheres offer the remarkable opportunity to study convection also under optically thin conditions. We roughly separate the models into a optically thin and thick part and derive the corresponding mixing-length parameters suitable to fit the hydrodynamical structures in the different regions. The mixing-length parameter of the optically thick region is most relevant for global stellar structure models, while the one of the optically thin part is most relevant for stellar atmospheres.

The entropy gradients of hydrodynamical and hydrostatic models correspond closely in the highest, convectively stable layers (with $\frac{ds}{d\tau} < 0$). By construction the standard models are in radiative equilibrium in these layers. This indicates that in the hydrodynamical models overshooting and wave heating are not particularly efficient, i.e. in the hydrodynamical models these layers are also close to radiative equilibrium. In the convectively unstable layers (with $\frac{ds}{d\tau} > 0$) the situation is markedly different. The stratifications (except for the log g=5.0 model which is close to convective equilibrium, i.e. almost adiabatically stratified) are neither close to radiative nor convective equilibrium. The

https://doi.org/10.1017/S0074180900133303 Published online by Cambridge University Press

detailed balance between radiative and convective energy transport determines the thermal structure. This makes the stratification sensitive to the values of the mixing-length parameter which provides a measure of the efficiency of the convective energy transport. As indicated in Fig. 8 we find a mixing-length parameter between 2.1 and 2.8 in the optically thin regions, and between 1.5 and 1.9 in the optically thick region. The extreme values of 1.5 and 2.1 are found in the $\log g$=5.0 model and are somewhat uncertain due to low sensitivity to changes of the mixing-length parameter. The $T_{\rm eff}$=3280 K and $\log g$=4.0 model (not plotted) shows values of 2.8 (optically thin part) and 2.2 (optically thick part).

Besides the detailed quantitative results two aspects are apparent: Firstly, it is not possible the specify a unique mixing-length parameter fitting the hydrodynamical stratification over the whole depth range. This illustrates principal shortcomings in the MLT. Secondly, the derived mixing-length parameters are falling in the range commonly considered. If one does not have high demands on the accuracy MLT provides a reasonable scaling of the energy transport efficiency with a fixed — perhaps solar calibrated — mixing-length parameter in the regime of M-type atmospheres.

## 6. Final remarks

While our results do not apply to the brown dwarf regime directly, it is tempting to extrapolate the mixing properties we found in our mid M-type objects. Our coolest and highest gravity model points towards a modest extra mixing by convective overshoot in brown dwarf atmospheres. The mixing would stay confined to layers in vicinity of the Schwarzschild stability boundary, and would not lead to a complete distribution of dust in the atmosphere (see LAH for more details).

Mixing-length theory does perform reasonably well in M-type atmospheres. To get a better quantitative description one might try to calibrate beside $\alpha_{\rm MLT}$ the "internal" parameters of MLT. M-type atmospheres appear particularly well suited for this undertaking since convection takes place under optically thick and thin conditions.

We reiterate that our results apply to atmospheres of solar metallicity. We expect a markedly different outcome for metal poor atmospheres.

**Acknowledgments.** This project benefitted from financial support of the Walter Gyllenberg Foundation, and the Swedish Vetenskapsrådet.

## 7. Discussion

GUSTAFSSON: The correction in the optically thin layer in your M-star models presumably due to H$\alpha$ formation lowering the adiabatic gradient, could significantly affect the bisectors for cores of relatively strong lines, as compare with solar spectra - Have you studied this, as yet?
LUDWIG: This is an interesting idea, but I have not done any spectral line synthesis yet. Indeed, the significantly different behavior of the velocity field in the optically thin regions might lead to qualitative differences.

## References

Allard, F., Hauschildt, P.H., & Schwenke, D., 2000, ApJ, 540, 1005

Baraffe, I., Chabrier, G., Allard, F., & Hauschildt, P.H., 2002, A&A, 382, 563

Freytag, B., Ludwig, H.-G., & Steffen, M., 1996, A&A, 313, 397

Hauschildt, P.H., & Baron, E., Journal of Computational and Applied Mathematics, 102, 41

Ludwig, H.-G., & Nordlund, Å., 2000: in: *Stellar Astrophysics*, Proceedings of the Pacific Rim Conference 1999, eds. K.S. Cheng, H.F. Chau, K.L. Chan, & K.C.Leung (Kluwer Academic Publishers), 37

Ludwig, H.-G., Allard, F., & Hauschildt, P.H., 2002, A&A, in press

Miesch, M.S., Brandenburg, A., & Zweibel, E.G., 2000, Phys. Rev. E, 61, 457

Mihalas, D., 1978, *Stellar Atmospheres* (Freeman and Company)

Steffen, M., Ludwig, H.-G., & Freytag, B., 1995, A&A, 300, 473

Stein, R.F., & Nordlund, Å., 1998, ApJ, 499, 914

Title, A.M., Tarbell, T.D., Topka, K.P., Ferguson, S.H., & Shine, R.A., 1989, ApJ, 336, 475